

## Determination of Formal Potentials of Multihemoprotein, Cytochrome $c_3$ by $^1\text{H}$ Nuclear Magnetic Resonance

Keisaku KIMURA,\* Shinsuke NAKAJIMA,<sup>†</sup> Katsumi NIKI,<sup>†</sup> and Hiroo INOKUCHI

*Institute for Molecular Science, Myodaiji, Okazaki 444*

<sup>†</sup>*Department of Electrochemistry, Yokohama National University, Tokiwadai, Hodogaya-ku, Yokohama 240*

(Received November 2, 1984)

Macroscopic redox potentials of tetrahemoprotein, cytochrome  $c_3$  from *D. vulgaris*, Miyazaki strain, were derived from 400 MHz  $^1\text{H}$  NMR measurements. The formal potential,  $E_1'$ , was determined to be  $-0.245 \pm 0.005$  V vs. NHE compared with a value of  $-0.240$  V obtained electrochemically. The distributions of the intermediate states from the NMR spectra during a redox titration are in good agreement with those previously determined by electrochemistry.

Cytochrome  $c_3$  (cyt.  $c_3$ ) has four hemes within a single polypeptide chain and functions as an electron carrier in the sulfate reducing bacteria, *Desulfovibrio vulgaris*. The oxidoreduction of cyt.  $c_3$  is regulated by the catalytic action of hydrogenase, an iron–sulfur enzyme. The physicochemical properties of the cyt.  $c_3$  have been well studied by Mössbauer spectroscopy,<sup>1)</sup> photoelectron spectroscopy,<sup>2)</sup> electrical conductivity,<sup>3)</sup> electrochemical methods,<sup>4,5)</sup> ESR,<sup>6)</sup> and NMR.<sup>7)</sup> These studies have revealed that this protein has unusual properties such as a very low ionization potential, high electrical conductivity, and a rapid and reversible redox reaction owing to its multiheme structure. It also has been suggested that the redox potentials of the hemes are connected with these properties.

The macroscopic redox potentials of this multihemeprotein derived from 400 MHz  $^1\text{H}$  NMR measurements are reported. These potentials have previously been obtained by the simulation of the differential pulse voltammetric response during redox titrations. The redox potential,  $E$ , of cyt.  $c_3$  is defined by

$$E = E_{i+1}^{\circ'} + (RT/F) \ln[f_i]/[f_{i+1}] \quad (1)$$

where  $E_{i+1}^{\circ'}$  is the macroscopic formal potential for the  $f_i \rightleftharpoons f_{i+1}$  equilibrium and where  $f_i$  is the  $i$ th oxidation state as shown in Fig. 1. It should be noted in this figure that there is an unity (one electron) difference for each oxidation state. There are five states corresponding to  $n=0, 1, 2, 3$ , and 4 electrons (designated by  $f_0$  to  $f_4$ ) while states  $f_1$ – $f_3$  can have multiplicities arising from the multicomponent electron sites.

### Experimental

*D. vulgaris* cyt.  $c_3$  was purified by a method previously reported.<sup>8)</sup> The purity index [ $A_{552}(\text{Fe}^{2+})/A_{280}(\text{Fe}^{3+})$ ] was 3.0. The protein was lyophilized twice from 99.95%  $\text{D}_2\text{O}$ . Hydrogenase was also purified according to the method described by Yagi *et al.*<sup>9)</sup> The lyophilized powder of cyt.  $c_3$  and a trace amount of deuterized hydrogenase were dissolved into the deuterized phosphate buffer solution ( $\text{pD}=7.0$ ), giving a final cyt.  $c_3$  concentration of 5 mM (1 M=1 mol  $\text{m}^{-3}$ ). The  $\text{pD}$  values were measured by a pH meter. The NMR spectra were recorded and analyzed using a JEOL GX 400 spec-

trometer. After measurements on the ferricytochrome  $c_3$ , it was reduced to the ferro-form by hydrogen. The samples of various intermediate oxidation states were prepared by the reoxidation of the fully reduced sample with air. All measurements were conducted at  $(25 \pm 0.5)^\circ\text{C}$ , and the chemical shifts were quoted in part per million, down field from sodium 3-(trimethylsilyl) propionate-2,2,3,3- $d_4$ (TSS).

The optical absorption spectra of the ca. 0.1 mM cyt.  $c_3$  of an intermediate oxidation state were measured in the NMR tube before and after NMR measurement. We confirmed that there were no significant differences in the optical spectra taken before and after NMR measurement. In the case of the 0.1 mM cyt.  $c_3$  solution, the number of accumulation of free induction decay was 10,000 in order to increase the signal to noise ratio. However, this acquisition number was still not large enough for a good signal to noise ratio and a smoothing technique was used to analyze the NMR lineshape.

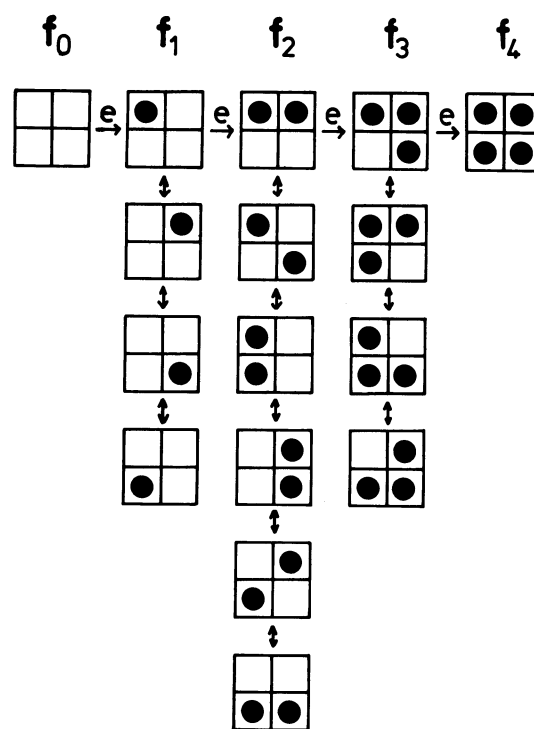


Fig. 1. Microscopic oxidation states of cyt.  $c_3$ . Solid circles indicate the reduced sites.  $f_0$ – $f_4$  indicate macroscopic oxidation states.

## Results and Discussion

Figure 2 shows the NMR spectra in the lower field region for a redox titration of cyt.  $c_3$ . The sharp singlet peaks (A—P) with three-proton intensity in the region of 31–8 ppm were assigned to the heme methyl resonances of the  $f_0$  state.<sup>7,10</sup> As the amount of reduction is incrementally increased, (spectra # 1–9 in Fig. 2) new peaks are seen to appear at the expense of the  $f_0$  intensity. The height of all  $f_0$  peaks decreased simultaneously. This is due to the fact that the intramolecular electron-exchange rate of cyt.  $c_3$  is so rapid on the NMR time scale that the microscopic states in each intermediate oxidation state,  $f_1$ ,  $f_2$ , and  $f_3$ , are indistinguishable, so it is the average fraction of each intermediate state that is determined by the NMR. From the intensity of five well-isolated peaks (A,B,C,F,I), the reduction ratio of the  $f_0$  state was obtained. The new peaks that appeared at 27.7,

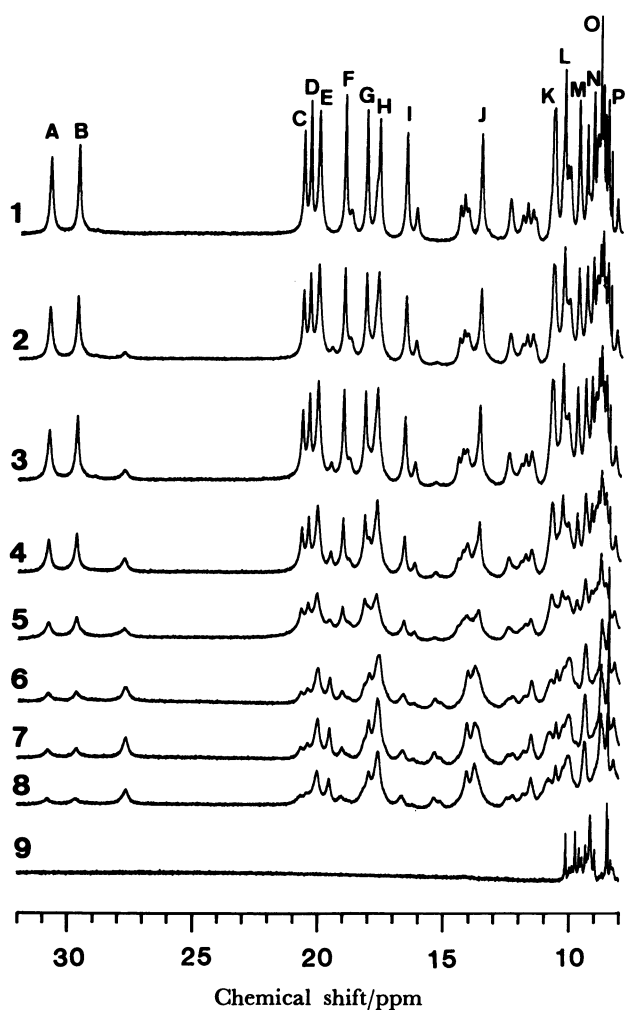


Fig. 2. NMR spectra for a redox titration of cyt.  $c_3$  recorded on a 400 MHz NMR: spectrum (1) is fully oxidized cytochrome  $c_3$ , (2)  $f_0=0.94$ , (3)  $=0.93$ , (4)  $=0.665$ , (5)  $=0.42$ , (6)  $=0.22$ , (7)  $=0.16$ , (8)  $=0.10$ , and (9) is fully reduced cyt.  $c_3$ .

20.0, 19.55, and 18.0 ppm were assigned to  $f_1$ , and those at 15.36, 14.1, and 13.8 ppm were assigned to  $f_2$ . The assignment was done by the saturation transfer method.<sup>7</sup>

From the peak area of each of the oxidation states, one can calculate the fractions of the  $f_0$ ,  $f_1$ , and  $f_2$  states. The macroscopic formal potential,  $E_1^{\circ'}$  for the equilibrium between  $f_0$  and  $f_1$ , can be determined from the ratio of the  $f_0$  state to the  $f_1$  state and was estimated to be  $(-0.245 \pm 0.005)$  V, which is in good agreement with that determined by the electrochemical method,  $-0.239$  V, in  $D_2O$ . Similarly, one can calculate the macroscopic formal potentials of the intermediate states from the fraction of each intermediate state.

The macroscopic formal potentials of cyt.  $c_3$  from *D. vulgaris* determined by electrochemical method in both  $H_2O$  and  $D_2O$  are given in Table 1. On the basis of the macroscopic formal potentials given in Table 1, we can calculate the relative concentrations of the five redox states defined in Fig. 1 as a function of the electrochemical potential as shown in Fig. 3. In the upper part of this figure, arrows designate the points at which UV and redox titration measurements were conducted. At the bottom of the figure, the four macroscopic formal potentials are shown. The broken line indicates the average fraction of the ferri-heme in cyt.  $c_3$ , which is observed by optical absorption spectroscopy. The ratios,  $f_1/f_0$  and  $f_2/f_0$ , calculated from

TABLE 1. MACROSCOPIC FORMAL POTENTIALS OF CYTOCHROME  $c_3$ , *D. vulgaris*, MIYAZAKI STRAIN (V vs. NHE)

	in $D_2O$ (pD=7.1)	in $H_2O$ (pH=7.1)
$E_1^{\circ'}$	-0.239	-0.240
$E_2^{\circ'}$	-0.293	-0.297
$E_3^{\circ'}$	-0.310	-0.315
$E_4^{\circ'}$	-0.352	-0.357

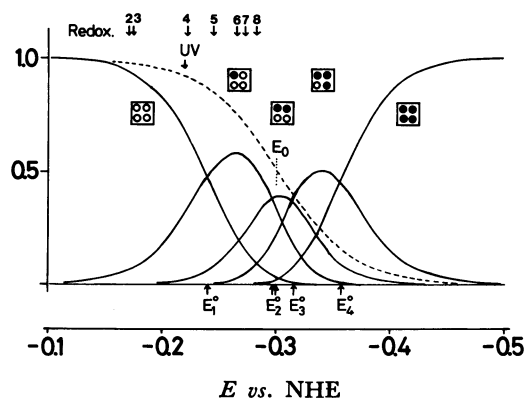


Fig. 3. Population of five macroscopic oxidation states calculated from the electrochemical data as a function of electrochemical potentials. Arrows on the top of the figure designate the intermediate oxidation states (2) to (8) shown in Fig. 2.

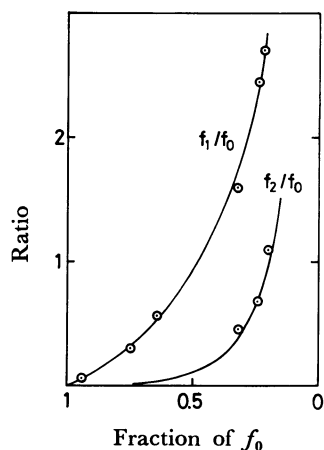


Fig. 4. The  $f_1/f_0$  and  $f_2/f_0$ , as a function of the fraction of the  $f_0$  state. Open circles are calculated from NMR data; solid lines, from electrochemical data.

the NMR data (open circles) and those from the data shown in Fig. 3 (solid lines) are plotted in Fig. 4 as a function of the fraction of the  $f_0$  state. The NMR data fit well with the curve calculated from electrochemical methods. These results strongly suggest that the four macroscopic formal potentials of the cyt.  $c_3$  are a unique set of formal potentials. The well resolved spectra in the present study gave the rigid foundation to assign the absorption lines, many of which were compatible with the early work.<sup>7)</sup> Based upon their poorly resolved spectra,<sup>11)</sup> Santos *et al.* derived four redox potentials of *D. gigas* which were quite different from the present study.

With respect to the reaction scheme between the microscopic states as shown in Fig. 1, we should emphasize that the intramolecular and intermolecular electron exchange rates and the microscopic formal potentials of cyt.  $c_3$  must be studied. Further NMR studies are now in progress.

This work was supported by Grant-in-Aid for Spe-

cial Project Research from the Ministry of Education, Science and Culture of Japan (No. 57102011) for which the authors would like to express their sincere thanks. Many useful discussions with Professor Ted Kuwana and Mrs. Jane Kuwana are gratefully acknowledged. The authors wish to acknowledge the kindly supply of sulfate reducing bacteria by Ajinomoto Co. as well as their continuous interest and help.

#### References

- 1) K. Ono, K. Kimura, T. Yagi, and H. Inokuchi, *J. Chem. Phys.*, **63**, 1640 (1975); M. Utuno, K. Ono, K. Kimura, H. Inokuchi, and T. Yagi, *ibid.*, **72**, 2264 (1980).
- 2) K. Kimura, N. Sato, S. Hino, T. Yagi, and H. Inokuchi, *J. Am. Chem. Soc.*, **100**, 6564 (1978); N. Sato, K. Kimura, H. Inokuchi, and T. Yagi, *Chem. Phys. Lett.*, **73**, 35 (1980).
- 3) Y. Nakahara, K. Kimura, H. Inokuchi, and T. Yagi, *Chem. Lett.*, **1979**, 877; K. Kimura, Y. Nakahara, T. Yagi, and H. Inokuchi, *J. Chem. Phys.*, **70**, 3317 (1979); K. Kimura and H. Inokuchi, *J. Phys. Soc. Jpn.*, **51**, 2218 (1982).
- 4) K. Niki, T. Yagi, H. Inokuchi, and K. Kimura, *J. Am. Chem. Soc.*, **101**, 3335 (1979).
- 5) W. Sokol, D. H. Evans, K. Niki, and T. Yagi, *J. Electroanal. Chem.*, **108**, 107 (1980); K. Niki, Y. Kobayashi, and H. Matsuda, *J. Electroanal. Chem.* in press.
- 6) J. LeGall, M. H. Bruschi and D. V. DerVartanian, *Biochim. Biophys. Acta*, **234**, 499 (1971); D. V. DerVartanian and J. LeGall, *ibid.*, **346**, 79 (1974).
- 7) J. J. G. Moura, H. Santos, I. Moura, J. LeGall, G. R. Moore, R. J. P. Williams, and A. V. Xavier, *Eur. J. Biochem.*, **127**, 151 (1982).
- 8) T. Yagi and K. Maruyama, *Biochim. Biophys. Acta*, **234**, 214 (1971).
- 9) T. Yagi, K. Kimura, H. Daidoji, F. Sakai, S. Tamura, and H. Inokuchi, *J. Biochem.*, **79**, 661 (1976).
- 10) In Ref. 7), only five of the sixteen heme methyls were assigned.
- 11) H. Santos, J. J. G. Moura, I. Moura, J. LeGall, and A. V. Xavier, *Eur. J. Biochem.*, **141**, 283 (1984).